Progress In Electromagnetics Research C, Vol. 33, 157–169, 2012

ANALYSIS OF LOSSY SIW STRUCTURES BASED ON THE PARALLEL PLATES WAVEGUIDE GREEN'S FUNCTION

G. Amendola*, E. Arnieri, and L. Boccia

Dipartimento di Elettronica, Informatica e Sistemistica, Università della Calabria, Rende (CS) 87036, Italy

Abstract—In this paper, a full-wave analysis technique of lossy substrate integrated waveguides, based on the dyadic Green's function of the parallel plate waveguide, is presented. The field inside the waveguide is expressed in terms of cylindrical vector wave-functions and the finite conductivity of the top and of the bottom plates, and of the metallic vias are taken into account. Losses into the dielectric substrate are also included. Coaxial ports are considered as sources and self and mutual admittances are evaluated. Cases of practical structure taken from literature are presented showing a very good agreement with the most used commercial software.

1. INTRODUCTION

The analysis of substrate integrated waveguide (SIW) [1] structures can be efficiently tackled using commercially available software packages. In fact, a considerable number of SIW based devices designed using commercial codes, like HFSS (Ansys HFSS), have been presented over the years. Filters [2–4, 23, 24], power dividers [5–7], antennas [8, 9, 25] and other devices have been successfully designed and realized. However, more effective analysis methods can be devised implementing techniques that, even less general than the one used in commercial codes, are more efficient in terms of both CPU time and occupied memory. Recently, several techniques have been proposed that may significantly shorten the design and optimization process. In [10] the Boundary Integral Resonant Modes Expansion (BIRME) has been adapted to analyze efficiently post walled structures, in [11–13] SIWs have been analyzed considering only the presence of the parallel plate

Received 16 August 2012, Accepted 7 October 2012, Scheduled 8 October 2012

* Corresponding author: Giandomenico Amendola (amendola@deis.unical.it).

waveguide (PPW) TEM mode and taking into account the scattering by the metallic posts, so reducing the analysis to the solution of a two dimensional problem. In [14] the authors presented a technique based on the full dyadic Green's function of the parallel plate, expressed as series of vector wave functions [16] *TE* and *TM* with respect to the waveguide height. In this last case also, the presence of the metallic vias was included in the analysis solving the scattering problem. The method was also used to determine the characteristics of SIW resonators [17] and to analyze SIW based slot arrays [18]. In this paper we present the extension of the technique presented in [14], which treated only lossless case, to lossy structures. To evaluate the power dissipated on the metallic surfaces and in the dielectric slab, the dyadic Green's function is changed to take into account the finite conductivity of the metallic plates [19] and including the dielectric losses into the argument of the wave functions. Furthermore, metallic posts are considered to have finite conductivity. As it is well known, for perfectly conducting cylinders, *TE* and *TM* mode do not couple. When a *TE* (or a *TM*) wave impinges on a perfectly conducting cylinder a *TE* (or a *TM*) field is scattered by the cylinder. For a finite conductivity cylinder or, more in general, for an impedance cylinder, this is no more true. However if a cylinder is made of a good conductor, as it is the case in this paper, the coupling between *TE* and *TM* waves can be neglected. This approximation makes the analysis considerably simpler and, as it will be shown, is valid in the case of SIW.

In this paper, the dyadic Green's function of the lossy parallel plate waveguide is firstly described. The complete derivation of the Green's function has been given in [14] but in this paper a slightly different path starting from the lossless case in [14] and relying on [15] is followed. The scattering by the lossy metallic cylinder, is considered later and added to the contribution from PPW. The most useful case of probe feeding is considered and results from passive devices already presented in literature are presented and discussed.

2. DYADIC GREEN'S FUNCTION OF THE LOSSY PARALLEL PLATES WAVEGUIDE

Following the notation in [14], the dyadic Green's function is expressed in the spectral domain as a series of cylindrical wave functions

$$\bar{\bar{\mathbf{G}}}_{\mathrm{PPW}} = \frac{j}{4\pi} \sum \int_0^\infty dk_\rho k_\rho \left[\frac{\mathbf{M}_n(k_\rho, \pm k_{0z}, \boldsymbol{\rho}, z)\mathbf{M}_{-n}(k_\rho, \mp k_{0z}, \boldsymbol{\rho}', z')}{k_{0z}k_\rho^2} + \frac{\mathbf{N}_n(k_\rho, \pm k_{0z}, \boldsymbol{\rho}, z)\mathbf{N}_{-n}(k_\rho, \mp k_{0z}, \boldsymbol{\rho}', z')}{k_{0z}k_\rho^2} \right] - \frac{\hat{z}\hat{z}\delta(\mathbf{r}-\mathbf{r}')}{\mathbf{k}_0^2} \qquad (1)$$

where $k_0 = \omega\sqrt{\mu_0(\varepsilon' + j\varepsilon'')}$, $k_{0z} = \sqrt{k_0^2 - k_\rho^2}$ and

$$\begin{aligned} \mathbf{M}_n = (k_\rho, k_{0z}, \boldsymbol{\rho}, z) &= \nabla \times \left(\Phi_n(k_\rho, \rho, \phi) e^{-jk_{0z}z}\hat{\mathbf{z}}\right) \\ \mathbf{N}_n = (k_\rho, k_{0z}, \boldsymbol{\rho}, z) &= \nabla \times \nabla \times \left(\Phi_n(k_\rho, \rho, \phi) e^{-jk_{0z}z}\hat{\mathbf{z}}\right) \end{aligned} \tag{2}$$

with

$$\Phi_n(k_\rho, \rho, \phi) = J_n(k_\rho \rho) e^{-jn\phi} \tag{3}$$

The free space Green's function is then used to find the Green's function of the parallel plate considering the field reflected from the conducting plates expanded in terms of the same vector eigenfunctions. This procedure, clearly described in [15], leads to

$$\begin{aligned} &\bar{\bar{\mathbf{G}}}_{\mathrm{PPW}} \\ &= -\frac{j}{4\pi}\sum\int_0^\infty dk_\rho k_\rho \times \left[(\nabla\times\hat{\mathbf{z}})(\nabla'\times\hat{\mathbf{z}})\frac{\Phi_n(k_\rho,\rho,\phi)\Phi_{-n}(k_\rho,\rho',\phi')}{k_z k_\rho^2} F_\pm^{TM}(z,z')\right. \\ &\left. + (\nabla\times\nabla\times\hat{\mathbf{z}})(\nabla'\times\nabla'\times\hat{\mathbf{z}})\frac{\Phi_n(k_\rho,\rho,\phi)\Phi_{-n}(k_\rho,\rho',\phi')}{k_z k_\rho^2} F_\pm^{TE}(z,z')\right] \\ &- \frac{1}{k^2}\hat{\mathbf{z}}\hat{\mathbf{z}}\delta(\mathbf{r}-\mathbf{r}') \end{aligned} \tag{4}$$

where

$$\begin{aligned} &F_\pm^{TM}(z,z') \\ &= \frac{\left(e^{jk_z z'} + e^{-jk_z z'} R_{TM}\right)\left(e^{-jk_z z} + e^{jk_z(z-2d)} R_{TM}\right)}{1 - R_{TM}^2 e^{-j2k_z d}} \quad \text{for } z > z' \\ &F_-^{TM}(z,z') = F_+^{TM}(z,z') \quad \text{for} \quad z < z' \end{aligned} \tag{5}$$

$F_\pm^{TE}(z, z')$ is derived from $F_\pm^{TM}(z, z')$ substituting R_{TM} with R_{TE} with [19]

$$R_{TM} = \frac{\varepsilon_c k_z - \varepsilon k_{2z}}{\varepsilon_c k_z + \varepsilon k_{2z}} \quad R_{TE} = \frac{k_z - k_{2z}}{k_z + k_{2z}} \tag{6}$$

and $k_{2z} = \sqrt{k_c^2 - k_\rho^2}$, $k_{2z} = \sqrt{k^2 - k_\rho^2}$. The previous expression are derived considering the top and bottom conducting plates as layers with dielectric constant $\varepsilon_c = -j\sigma/\omega$ [19].

The spectral integral in (4) is now solved by extending the integration limits to $[-\infty, +\infty]$ introducing Hankel's functions and applying the residue theorem [19]. One obtains

$$\bar{\bar{\mathbf{G}}}_{\mathrm{PPW}} \cdot \bar{\bar{I}}_t = -\frac{1}{4}\left[\sum\nolimits_{nm} \frac{\mathbf{M}_n(k_{\rho m}, k_{zm}, \rho, z, 2d)\mathbf{M}_{-n}(k_{\rho m}, -k_{zm}, \rho', z', 0)}{D^{TM'}(k_{\rho m})}\right.$$

$$+\frac{\mathbf{N}_n(k_{\rho m},k_{zm},\rho,z,2d)\mathbf{N}_{-n}(k_{\rho m},-k_{zm},\rho',z',0)}{D^{TE\prime}(k_{\rho m})}\Bigg]\cdot\bar{\bar{I}}_t \quad z>z' \tag{7}$$

$$\bar{\bar{\mathbf{G}}}_{\mathrm{PPW}}\cdot\bar{\bar{I}}_t=-\frac{1}{4}\Bigg[\sum_{nm}\frac{\mathbf{M}_n(k_{\rho m},-k_{zm},\rho,z,2d)\mathbf{M}_{-n}(k_{\rho m},k_{zm},\rho',z',0)}{D^{TM\prime}(k_{\rho m})}$$
$$+\frac{\mathbf{N}_n(k_{\rho m},-k_{zm},\rho,z,2d)\mathbf{N}_{-n}(k_{\rho m},k_{zm},\rho',z',0)}{D^{TE\prime}(k_{\rho m})}\Bigg]\cdot\bar{\bar{I}}_t \quad z<z' \tag{8}$$

In the previous expressions the transverse components are selected by means of the scalar product with the transverse dyad $\bar{\bar{I}}_t$, d is the height of the parallel plate and the quantity, $k_{\rho m}$ is evaluated as residues of integral (4) [19], $k_{zm}=\sqrt{k^2-k_\rho^2}$ and $\mathbf{M}_n$ and $\mathbf{N}_n$ functions have the following expressions

$$\mathbf{M}_n(k_{\rho m},k_{zm},\rho_{<>},z,\Delta z)$$
$$=(\nabla\times\hat{\mathbf{z}})\begin{Bmatrix}J_n(k_{\rho m}\rho_<)\\H_n^{(2)}(k_{\rho m}\rho_>)\end{Bmatrix}\times e^{-jn\phi}\left(e^{-jk_{zm}z}+e^{jk_{zm}(z-\Delta z)}R_{TM}\right) \tag{9}$$

$$\mathbf{N}_n(k_{\rho m},k_{zm},\rho_{<>},z,\Delta z)$$
$$=\frac{1}{k}(\nabla\times\nabla\times\hat{\mathbf{z}})\begin{Bmatrix}J_n(k_{\rho m}\rho_<)\\H_n^{(2)}(k_{\rho m}\rho_>)\end{Bmatrix}\times e^{-jn\phi}\left(e^{-jk_{zm}z}+e^{jk_{zm}(z-\Delta z)}R_{TE}\right) \tag{10}$$

where $\rho_>=\max(\rho,\rho')$, $\rho_<=\min(\rho,\rho')$. Furthermore, $D^{TE\prime}$ and $D^{TM\prime}$ are the derivative with respect to k_ρ of

$$\begin{aligned}D^{TM}&=k_{0z}k_\rho\left(1-R_{TM}^2e^{-j2k_zd}\right)\\D^{TE}&=k_{0z}k_\rho\left(1-R_{TE}^2e^{-j2k_zd}\right)\end{aligned} \tag{11}$$

3. SCATTERING FROM METALLIC VIAS OF FINITE CONDUCTIVITY

As pointed out in the introduction, to evaluate the scattering by impedance cylinders one has to consider both *TE* and *TM* fields

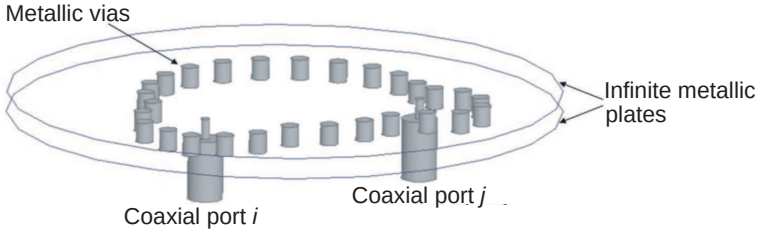

Figure 1. General geometry of a SIW structure with coaxial ports.

independently from the nature of the exciting field. However, as is known, vias are made of good conductor and one can consider that they scatter mostly TM (TE) field when the impinging field is TM (TE) and that the TE (TM) field is negligible. Under this hypothesis the scattering from metallic vias is taken into account as in [14] but enforcing the following boundary conditions on the cylinders surface:

$$\hat{\boldsymbol{\rho}} \times \nabla \times \mathbf{H} = -j\omega\varepsilon_r\varepsilon_0 Z_s \mathbf{H} \tag{12}$$

with

$$Z_s = (1+j)\sqrt{\frac{\omega\mu_0}{2\sigma}} \tag{13}$$

The field scattered from vias is expressed as series of outgoing TM and TE waves centered on cylinders

$$\begin{aligned} \mathbf{H}_{sCyl} \;=\; & \sum\nolimits_l \sum\nolimits_{n,m} \mathbf{M}_n(k_{\rho m}, k_{zm}, \boldsymbol{\rho} - \boldsymbol{\rho}_l, z, 2d) A^M_{m,n,l} \\ & + \sum\nolimits_{n,m} \mathbf{N}_n(k_{\rho m}, k_{zm}, \boldsymbol{\rho} - \boldsymbol{\rho}_l, z, 2d) A^N_{m,n,l} \end{aligned} \tag{14}$$

where (see Figure 2) l is an index spanning over the cylinders, m and n are relevant to vertical and angular dependencies, $\boldsymbol{\rho}_l$ is the position of the center of the cylinder l, and $A^M_{m,n,l}$, $A^N_{m,n,l}$ are unknown coefficients to be determined.

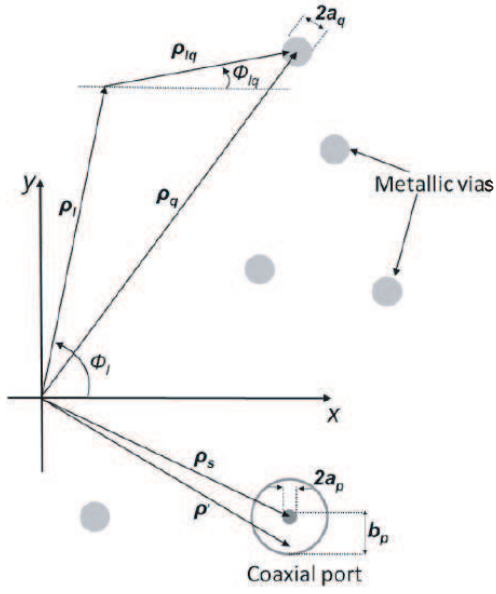

Figure 2. Coordinate system.

As it was done in [14], for any cylinder q one has the following equations, one for the TM mode one for the TE modes corresponding to apex M and N, respectively:

$$\begin{aligned} \Gamma^{M,N}_{q,r,m} &= \sum\nolimits_{l\neq q}\sum\nolimits_{n} L^{M,N}_{q,r,m,l,n} A^{M,N}_{m,n,l} + A^{M.N}_{m,r,q} \\ L^{M,N}_{q,r,m,l,n} &= T^{M,N}_{r,m,q} H^{(2)}_{n-r}(k_{\rho m}\rho_{lq}) e^{-j(n-r)\phi_{lq}} \\ \Gamma^{M,N}_{q,r,m} &= -T^{M,N}_{r,m,q} v^{TM}_{r,m,q} \end{aligned} \tag{15}$$

where

$$\begin{aligned} T^{M,N}_{r,m,q} &= -\frac{J_r(k_{\rho m}a_q) + Z^{J,M}_m}{H^{(2)}_r(k_{\rho m}a_q) + Z^{H,M}_m} \\ Z^{J,M}_m &= \frac{j\omega\varepsilon_r\varepsilon_0}{k_{\rho m}} Z_s J'_r(k_{\rho m}a_q) \\ Z^{H,M}_m &= \frac{j\omega\varepsilon_r\varepsilon_0}{k_{\rho m}} Z_s H^{(2)'}_r(k_{\rho m}a_q) \end{aligned} \tag{16}$$

and

$$\begin{aligned} T^{M,N}_{r,m,q} &= \frac{J'_r(k_{\rho m}a_q) + Z^{J,M}_m}{H^{(2)'}_r(k_{\rho m}a_q) + Z^{H,N}_m} \\ Z^{J,N}_m &= \frac{k_{\rho m}}{j\omega\mu_0} Z_s J_r(k_{\rho m}a_q) \\ Z^{H,M}_m &= \frac{k_{\rho m}}{j\omega\mu_0} Z_s H^{(2)}_r(k_{\rho m}a_q) \end{aligned} \tag{17}$$

In the previous formulas $v^M_{r,m,q}$ and $v^N_{r,m,q}$ are expressed as

$$\begin{aligned} v^M_{r,m,q} &= \frac{j\omega\varepsilon_r\varepsilon_0}{4D^{TM'}(k_{\rho m})} \times \int d\mathbf{r}' \mathbf{M}_n\left(k_{\rho m}, -k_{zm}, \boldsymbol{\rho}' - \boldsymbol{\rho}_q, z', 0\right) \cdot \mathbf{J}_M\left(\mathbf{r}'\right) \\ v^N_{r,m,q} &= \frac{j\omega\varepsilon_r\varepsilon_0}{4D^{TE'}(k_{\rho m})} \times \int d\mathbf{r}' \mathbf{N}_n\left(k_{\rho m}, -k_{zm}, \boldsymbol{\rho}' - \boldsymbol{\rho}_q, z', 0\right) \cdot \mathbf{J}_M\left(\mathbf{r}'\right) \end{aligned} \tag{18}$$

and they the excitation coefficients of the field radiated into the parallel plate waveguide free of the metallic vias.

4. SELF AND MUTUAL ADMITTANCE OF COAXIALLY FED LOSSY SIW STRUCTURES

In this paper coaxial probes will be considered as sources, in this case [14] the TE modes are not excited and in the Green's function only the TM contribution is retained. Also the TE field scattered by the

cylinders do not couple with the probes and the expressions of the TM scattered field given in the previous section account for the contribution from metallic vias. Admittances are computed considering the reaction between ports as

$$Y^{(p_i,p_j)} = \frac{\int_{S_{p_j}} \mathbf{dr}\mathbf{H}^{p_i}(\mathbf{r}) \cdot \mathbf{J}_M^{p_j}(\mathbf{r})}{|V|^2} \tag{19}$$

where $\mathbf{H}^{p_i}(\mathbf{r})$ is the total magnetic field due to the current $\mathbf{J}_M^{p_i}(\mathbf{r})$ on port p_i and S_{p_j} is the area on port p_j on which flows the current $\mathbf{J}_M^{p_j}(\mathbf{r})$. Self-admittance has the following closed form expressions:

$$\begin{aligned}
&Y^{(p_i,p_j)}\\
&=-\frac{j\omega\varepsilon}{4\pi^2}\frac{1}{4}\frac{1}{\log\left(\frac{b_{pi}}{a_{pi}}\right)^2}\sum\nolimits_m \frac{1}{D^{TM'}(k_{\rho m})} I_m^{(1)}\Big(1+e^{-jk_{zm}2d}R_{TM}\Big)(1+R_{TM})\\
&+\sum\nolimits_m A_{m,0,l_i}^{M,p_i} I_m^{(2)}\Big(1+e^{-jk_{zm}2d}R_{TM}\Big)\\
&+\sum\nolimits_{l\neq l_i}\sum\nolimits_{n,m} I_m^{(3)}\Big(1+e^{-jk_{zm}2d}R_{TM}\Big)(-1)^n H_n^{(2)}(k_{\rho m}\rho_l)e^{-j\phi_l}A_{m,n,l}^{M,p_i}
\end{aligned} \tag{20}$$

where l_i is the index corresponding to probe p_i, $A_{m,n,l}^{M,p_i}$ are the coefficients relevant to cylinder l and due to the source p_i and [14]

$$\begin{aligned}
I_m^{(1)} =& \frac{2j}{\pi}\ln\left(\frac{b_{p_i}}{a_{p_i}}\right) - H_0^{(2)}(k_{\rho m}b_{p_i})\left[J_0(k_{\rho m}b_{p_i}) - J_0(k_{\rho m}a_{p_i})\right]\\
&+ J_0(k_{\rho m}a_{p_i})\left[H_0^{(2)}(k_{\rho m}b_{p_i}) - H_0^{(2)}(k_{\rho m}a_{p_i})\right]\\
I_m^{(2)} =& \frac{2\pi}{\ln\left(\frac{b_{p_i}}{a_{p_i}}\right)}\left[H_0^{(2)}(k_{\rho m}b_{p_i}) - H_0^{(2)}(k_{\rho m}a_{p_i})\right]\\
I_m^{(3)} =& \frac{2\pi}{\ln\left(\frac{b_{p_i}}{a_{p_i}}\right)}\left[J_0(k_{\rho m}b_{p_i}) - J_0(k_{\rho m}a_{p_i})\right]
\end{aligned} \tag{21}$$

Mutual admittance has the following expression

$$\begin{aligned}
&Y^{(p_j,p_i)}\\
&=-\frac{j\omega\varepsilon}{4\pi^2}\frac{1}{4}\frac{1}{\log\left(\frac{b_{p_i}}{a_{p_i}}\right)^2}\sum\nolimits_m \frac{1}{D^{TM'}(k_{\rho m})}\Big(1+e^{-jk_{zm}2d}R_{TM}\Big)(1+R_{TM})\\
&\times\left[J_0(k_{\rho m}b_{p_j}) - J_0(k_{\rho m}a_{p_j})\right]^2 H_0^{(2)}(k_{\rho m}\rho_{ji})\\
&+\sum\nolimits_m\Big[H_0^{(2)}(k_{\rho m}b_{p_j}) - H_0^{(2)}(k_{\rho m}a_{p_j})\Big](-1)^m A_{m,0,l_j}^{M,p_i}\Big(1+e^{-jk_{zm}2d}R_{TM}\Big)\\
&+\sum\nolimits_{\substack{l\neq l_j\\ n,m}}\left[J_0(k_{\rho m}b_{p_j}) - J_0(k_{\rho m}a_{p_j})\right]
\end{aligned}$$

$$\times(-1)^n H_0^{(2)}(k_{\rho m}\rho_{l_j})e^{-j\phi_{l_j}} A_{m,n,l}^{M,p_i}\left(1+e^{-jk_{zm}2d}R_{TM}\right) \tag{22}$$

in which p_{ij} is the distance between ports i and j.

5. RESULTS

The theory presented in the previous sections has been implemented in a MATLAB code. To check the accuracy of the method a simple SIW cavity has been simulated with HFSS and the MATLAB code and results compared with measurements. In Figure 3 are presented the scattering parameters of the cavity fed with two coaxial probes. As it can be seen the method presented in this paper gives results more accurate than HFSS which predicts a 50 MHz shift with respect to measured results. In Figure 4 a SIW post filter presented in [20] is analyzed. As waveguide ports have been used in HFSS simulations, the effects of the coaxial probes has been de-embedded similarly to what was done in [14]. To better appreciate the accuracy of the proposed method in Figure 5 is shown the S_{21} for the lossless and the lossy case. Results obtained with the method in this paper and HFSS are in a very good agreement. In Figures 6 and 7 two further examples are presented which show the scattering parameters of a single and dual circular SIW filters. The results for the single pole filter are coherent with

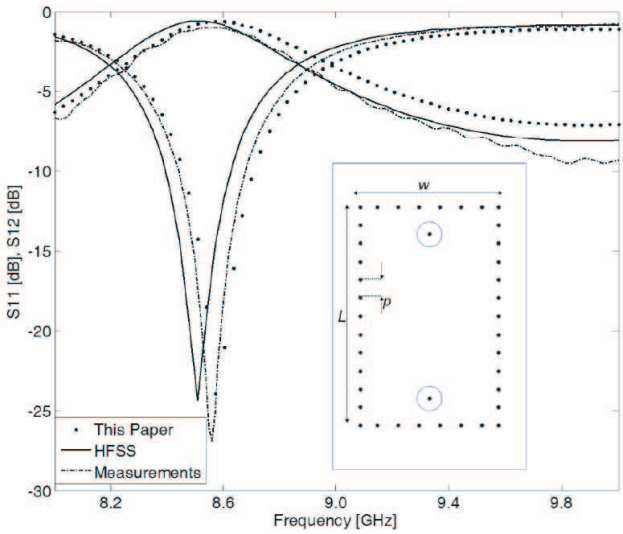

Figure 3. Substrate integrated waveguide cavity $w = 15.17\,\text{mm}$, $L = 24\,\text{mm}$, $p = 2\,\text{mm}$, $h = 0.787\,\text{mm}$, vias diameter $0.2\,\text{mm}$, $\varepsilon_r = 3.58$, $\tan\delta = 0.0035$, $\sigma = 5.8 * 10^7\,\text{S/m}$.

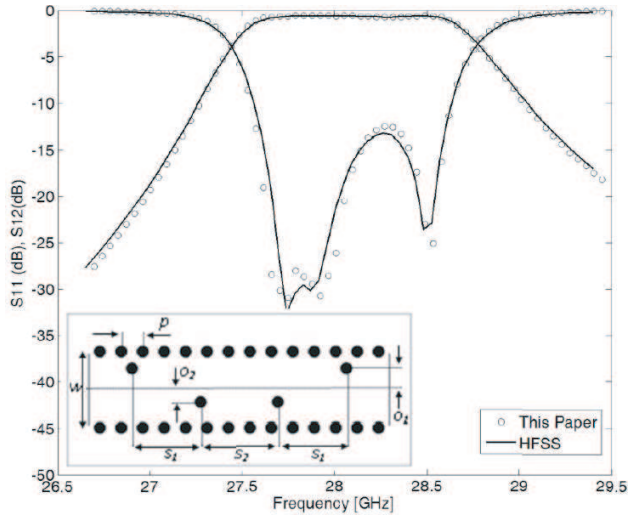

Figure 4. Substrate integrated waveguide post filter as in [20]. $w = 5.563\,\text{mm}$, $p = 1.525\,\text{mm}$, $o_1 = o_2 = 1.01\,\text{mm}$, $s_1 = 4.71\,\text{mm}$, $s_2 = 5.11\,\text{mm}$, $h = 0.787\,\text{mm}$, vias diameter $0.775\,\text{mm}$, $\varepsilon_r = 2.2$, $\tan\delta = 0.0011$, $\sigma = 5.8 * 10^7\,\text{S/m}$.

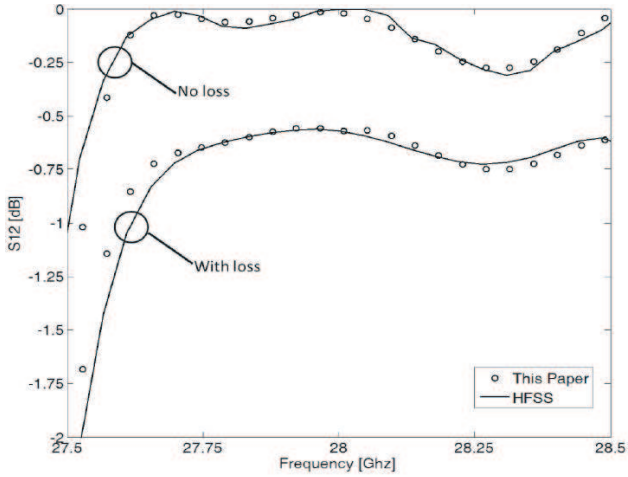

Figure 5. Insertion loss of the substrate integrated waveguide bandpass post filter presented in Figure 3 calculated with loss and without loss.

the resonator presented in Figure 1. In this case also HFSS predicts a slight frequency shift. For the more complex,two cavity filter results are in a good agreement.

The advantage of the method proposed in this paper over a general purpose software, like HFSS, is that the CPU time is considerably reduced. In fact, even if the structures presented in this paper are not

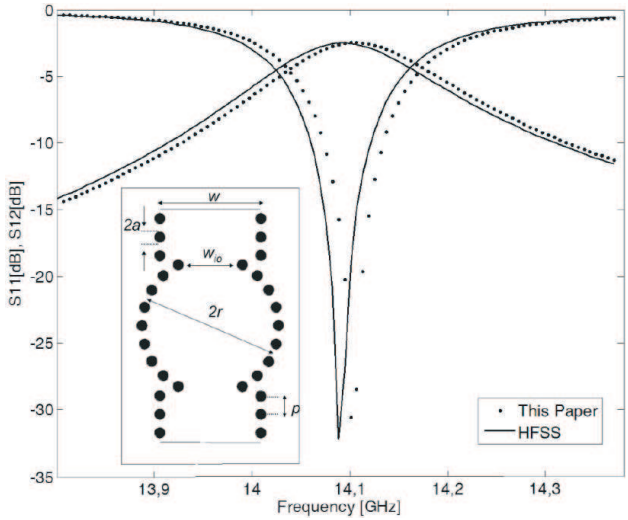

Figure 6. Scattering parameters of a single cavity circular filter, as in [21], $h = 0.380\,\text{mm}$, $w = 3.8\,\text{mm}$, $wio = 1.683\,\text{mm}$, $a = 0.2\,\text{mm}$, $r = 2.4\,\text{mm}$, $p = 0.7\,\text{mm}$, $\varepsilon_r = 9.9$, $\tan\delta = 0.001$, $\sigma = 5.8 * 10^7\,\text{S/m}$.

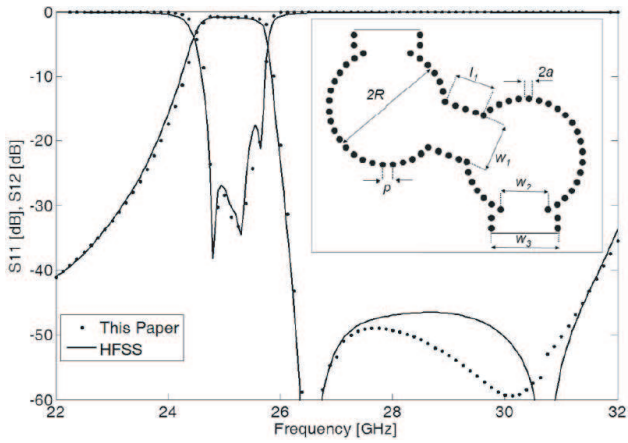

Figure 7. Scattering parameters of a dual-cavity filter as in [22], $h = 0.5\,\text{mm}$, $w_1 = 4.08\,\text{mm}$, $w_2 = 3.93\,\text{mm}$, $w_3 = 5.50\,\text{mm}$, $a = 0.2\,\text{mm}$, $p = 0.851\,\text{mm}$, $l_1 = 3.404\,\text{mm}$, $R = 4.83\,\text{mm}$, $a = 2.55\,\text{mm}$, $\varepsilon_r = 2.2$, $\tan\delta = 0.001$, $\sigma = 5.8 * 10^7\,\text{S/m}$.

very large, computational times are significantly shortened. A quad core Pentium at 2.4 GHz was used for this paper and CPU times do not differ much from the ones already presented in [18] for the lossless cases, as it seems that only one of the core is actively running. For this reason only CPU times for the largest structure are here reported. It has been found that HFSS required 146 seconds for the mesh set up and 9 seconds per frequency points to produce the results in Figure 7, while 2.6 seconds per frequency points were needed to the matlab code to perform the same simulation.

6. CONCLUSIONS

In this paper, an efficient semi-analytical method to analyze lossy SIW structures has been presented. The method is based on the dyadic Green's function of the parallel plates waveguide in which metallic vias are embedded. Coaxial probes were included in the model. Results compare well with HFSS results and measurements and they have been obtained with reduced computational resources.

REFERENCES

1. Deslandes, D. and K. Wu, "Integrated microstrip and rectangular waveguide in planar form," *IEEE Microwave and Wireless Components Letters*, Vol. 11, No. 2, 68–70, 2001.
2. Ismail, A., M. S. Razalli, M. A. Mahdi, R. S. A. Raja Abdullah, N. K. Noordin, and M. F. A Rasid, "X-band trisection substrate-integrated waveguide quasi-elliptic filter," *Progress In Electromagnetics Research*, Vol. 85, 133–145, 2008.
3. Zhang, Z. G., Y. Fan, Y. J. Cheng, and Y.-H. Zhang, "A novel multilayer dual-mode substrate integrated waveguide complementary filter with circular and elliptic cavities (SICC and SIEC)," *Progress In Electromagnetics Research*, Vol. 127, 173–188, 2012.
4. Wu, L.-S., J.-F. Mao, W. Shen, and W.-Y. Yin, "Extended doublet bandpass filters implemented with microstrip resonator and full-/half-mode substrate integrated cavities," *Progress In Electromagnetics Research*, Vol. 108, 433–447, 2010.
5. Kazemi, R., R. A. Sadeghzadeh, and A. E. Fathy, "Design of a wide band eight-way compact SIW power combiner FED by a low loss GCPW-to-SIW transition," *Progress In Electromagnetics Research C*, Vol. 26, 97–110, 2012.

6. Boccia, L., A. Emanuele, E. Arnieri, A. Shamsafar, and G. Amendola, "Substrate integrated power combiners," *Proceedings of 6th European Conference on Antennas and Propagation, EuCAP*, 3631–3634, 2012.
7. Wu, D., Y. Fan, M. Zhao, and B. Zheng, "Vertical transition and power divider using via walled circular cavity for multilayer millimeter wave module," *Journal of Electromagnetic Waves and Applications*, Vol. 23, Nos. 5–6, 729–735, 2009.
8. Djerafi, T. and K. Wu, "Corrugated substrate integrated waveguide (SIW) antipodal linearly tapered slot antenna array fed by quasi-triangular power divider," *Progress In Electromagnetics Research C*, Vol. 26, 139–151, 2012.
9. Amendola, G., E. Arnieri, L. Boccia, and V. Ziegler, "Annular ring slot radiating element for integrated millimeter wave arrays," *2012 6th European Conference on Antennas and Propagation (EUCAP)*, 3082–3085, Mar. 26–30, 2012.
10. Mira, F., A. San Blas, S. Cogollos, V. Boria, and B. Gimeno, "Computer-aided design of substrate integrated waveguide filters for microwave and millimeter-wave applications," *IEEE 2009 Eur. Microw. Conf. (EuMC 2009)*, 425–428, 2009.
11. Diaz Caballero, E., H. Esteban, A. Belenguer, and V. Boria, "Efficient analysis of substrate integrated waveguide devices using hybrid mode matching between cylindrical and guided modes," *IEEE Transactions on Microwave Theory and Techniques*, Vol. 60, No. 2, 232–243, Feb. 2012.
12. Wu, X. and A. Kishk, "Hybrid of method of moments and cylindrical eigenfunction expansion to study substrate integrated waveguide circuits," *IEEE Transactions on Microwave Theory and Techniques*, Vol. 56, No. 10, 2270–2276, Oct. 2008.
13. Abaei, E., E. Mehrshahi, G. Amendola, E. Arnieri, and A. Shamsafar, "Two dimensional multi-port method for analysis of propagation characteristics of substrate integrated waveguide," *Progress In Electromagnetics Research C*, Vol. 29, 261–273, 2012.
14. Arnieri, E. and G. Amendola, "Analysis of substrate integrated waveguide structures based on the parallel plate waveguide Green's function, " *IEEE Transactions on Microwave Theory and Techniques*, Vol. 56, No. 7, 1615–1623, Jul. 2008.
15. Chew, W. C., *Waves and Fields in Inhomogeneous Media*, IEEE Press, 1995.
16. Tsang, L., J. A. Kong, K. H. Ding, and C. Ao, *Scattering of Electromagnetic Waves: Numerical Simulations*, Wiley, 2001.

17. Amendola, G., G. Angiulli, E. Arnieri, and L. Boccia, "Resonant frequencies of circular substrate integrated resonators," *IEEE Microwave and Wireless Components Letters*, Vol. 18, No. 4, 239–241, Apr. 2008.
18. Arnieri, E. and G. Amendola, "Method of moments analysis of slotted substrate integrated waveguide arrays," *IEEE Transactions on Antennas and Propagation*, Vol. 59, No. 4, 1148–1154, Apr. 2011.
19. Huang, C.-C., L. Tsang, and C. H. Chan, "Multiple scattering among vias in lossy planar waveguides using SMCG method," *IEEE Transactions on Advanced Packaging*, Vol. 25, No. 2, 181–188, May 2002.
20. Bozzi, M., L. Perregrini, and K. Wu, "Modeling of conductor, dielectric, and radiation losses in substrate integrated waveguide by the boundary integral-resonant mode expansion method," *IEEE Transactions on Microwave Theory and Techniques*, Vol. 56, No. 12, 3153–3161, Dec. 2008.
21. Potelon, B., J.-C. Bohorquez, J.-F. Favennec, C. Quendo, E. Rius, and C. Person, "Design of ku-band filter based on substrate integrated circular cavities (SICCs)," *IEEE MTT-S Int. Microw. Symp.*, 1237–1240, San Francisco, CA, Jun. 2006.
22. Tang, H. J. and W. Hong, "Substrate integrated waveguide dual mode filter with circular cavity," *Joint Int. Conf. on Infrared Millimetre Waves and on Terahertz Electronics, IRMMW-THz*, 399–399, Shangai, Sep. 2006.
23. Zhang, Q.-L., W.-Y. Yin, S. He, and L.-S. Wu, "Evanescent-mode substrate integrated waveguide (SIW) filters implemented with complementary split ring resonators," *Progress In Electromagnetics Research*, Vol. 111, 419–432, 2011.
24. Wang, Z., X. Li, S. Zhou, B. Yan, R.-M. Xu, and W. Lin, "Half mode substrate integrated folded waveguide (HHSIFW) and partial H-plane bandpass filter," *Progress In Electromagnetics Research*, Vol. 101, 203–216, 2010.
25. Bakhtafrooz, A., A. Borji, D. Busuioc, and S. Safavi-Naeini, "Novel two-layer millimeter-wave slot array antennas based on substrate integrated waveguides," *Progress In Electromagnetics Research*, Vol. 109, 475–491, 2010.